A novel biological role for PADs: Citrullination of cathelicidin LL-37 controls the immunostimulatory potential of cell-free DNA

Alicia Wong[*], **Danuta Bryzek**[*], **Ewelina Dobosz**[*], **Carsten Scavenius**[†], **Pavel Svoboda**[‡], **Maria Rapala-Kozik**[§], **Adam Lesner**[¶], **Ivo Frydrych**[‖], **Jan Enghild**[†], **Piotr Mydel**[*,#], **Jan Pohl**[‡], **Paul R. Thompson**[**], **Jan Potempa**[*,††], and **Joanna Koziel**[*]

[*]Department of Microbiology, Faculty of Biochemistry, Biophysics and Biotechnology, Jagiellonian University, 30-387 Krakow, Poland [†]Interdisciplinary Nanoscience Center at the Department of Molecular Biology and Genetics, Aarhus University, 8000 Aarhus, Denmark [‡]Division of Scientific Resources, CDC, 30329-4027 Atlanta, Georgia, USA [§]Department of Comparative Biochemistry and Bioanalytics, Faculty of Biochemistry, Biophysics and Biotechnology, Jagiellonian University in Krakow, 30-387 Krakow, Poland [¶]Faculty of Chemistry, University of Gdansk, 80-309 Gdansk, Poland [‖]Institute of Molecular and Translational Medicine, Faculty of Medicine and Dentistry, Palacky University, 77126 Olomouc, Czech Republic [#]Broegelmann Research Laboratory, Department of Clinical Science, University of Bergen, 5020 Norway [**]Department of Biochemistry and Molecular Pharmacology, UMass Medical School, 01605-4321 Massachusetts, USA [††]Center for Oral Health and Systemic Disease, University of Louisville School of Dentistry, University of Louisville, 40202 Louisville, KY, USA

Abstract

LL-37, the only human cathelicidin which is released during inflammation, is a potent regulator of immune responses by facilitating delivery of oligonucleotides to intracellular TLR-9, thereby enhancing the response of human plasmacytoid dendritic cells (pDCs) to extracellular DNA. Although important for pathogen recognition, this mechanism may facilitate development of autoimmune diseases. Here, we show that citrullination of LL-37 by peptidyl-arginine deiminases (PADs) hindered peptide-dependent DNA uptake and sensing by pDCs. In contrast, carbamylation of the peptide (homocitrullination of Lys residues) had no effect. The efficiency of LL-37 binding to oligonucleotides and activation of pDCs was found to be inversely proportional to the number of citrullinated residues in the peptide. Similarly, preincubation of carbamylated LL-37 with PAD2 abrogated the peptide's ability to bind DNA. Conversely, LL-37 with Arg residues substituted by homoarginine, which cannot be deiminated elicited full activity of native LL-37 regardless of PAD2 treatment. Taken together, the data showed that citrullination abolished LL-37 ability to bind DNA and altered the immunomodulatory function of the peptide. Both activities were dependent on the proper distribution of guanidinium side chains in the native peptide sequence. Moreover, our data suggests that cathelicidin/LL-37 is citrullinated by PADs during NET formation, thus affecting the inflammatory potential of NETs. Together this may represent a novel

Corresponding authors: Joanna Koziel and Jan Potempa, Department of Microbiology, Faculty of Biochemistry, Biophysics and Biotechnology, Jagiellonian University, ul. Gronostajowa 7, 30-387 Krakow, Poland, joanna.koziel@uj.edu.pl; jan.potempa@louisville.edu, tel: +48126646377; fax: +48126646902.

mechanism for preventing the breakdown of immunotolerance, which is dependent on the response of antigen-presenting cells to self-molecules (including cell-free DNA); overactivation may facilitate development of autoimmunity.

Keywords

LL-37; dendritic cells; nucleic acids; TLR-9; citrullination; PADs; NETs

Introduction

Human antimicrobial peptide LL-37 (hCAP18) is the sole human member of the cathelicidin family. The mature cationic peptide, which comprises 37 amino acids, has two N-terminal leucine residues and is released from an 18-kDa precursor protein (cathelicidin) by protease-3 (1). Cathelicidin is abundant in intracellular granules of myeloid cells and is also produced locally in epithelial tissues (2,3). The biological effects of LL-37 (e.g., effects on the permeability of the microbial cell membrane or neutralization of LPS activity) (4) are dependent on the amphipathic, cationic nature of the peptide. A recent study shows that LL-37 also has several immunomodulatory functions that regulate host responses to pathogens (5). Moreover, LL-37 affects chemotaxis of immune cells, epithelial cell activation, angiogenesis, and epithelial wound repair.

Post-translational modification of LL-37 has a strong influence on its immunomodulatory functions (6). In particular, deimination plays a special role. Notably, the primary structure of LL-37 contains five arginine residues that are citrullinated by the peptidyl-arginine deiminases (PADs). PADs are calcium-dependent hydrolases that catalyze conversion of positively charged arginine to neutral citrulline (7). Mammals harbor five different PAD isoforms: PAD 1–4 and 6 (8). Previous findings highlight how PAD2 and PAD4, enzymes predominantly expressed in granulocytes, affect the biological activity of LL-37 (6,9). For example, citrullinated LL-37 is less efficient at neutralizing the proinflammatory activity of many TLR agonists; also, due to a marked reduction in its affinity for endotoxin, the modified peptide is unable to prevent endotoxin shock (9).

LL-37 forms complexes with negatively-charged oligonucleotides derived both from dying host cells and pathogens (10, 11, 12) and it is suggested that it can act as an oligonucleotide carrier that transports nucleic acids across the cell membrane into the endosomal compartment of myeloid cells, including antigen-presenting cells (APCs) (13). This mechanism increases recognition of bacterial DNA by intracellular receptors such as TLR-9, thereby stimulating the immune response. However, there is a downside in LL-37-mediated internalization of self-DNA to the endosomal compartment of plasmacytoid dendritic cells (pDCs) since it sensitizes antigen presenting host cells to self-antigens (10), leading to the breakdown of immune tolerance; this mechanism underlies the pathogenesis of autoimmune diseases such as systemic lupus erythematous (SLE) and rheumatoid arthritis (RA). One postulated mechanism involves accumulation of neutrophil extracellular traps (NETs) in which DNA fibers are coated by antimicrobial peptides (14). Following our previous findings showing that deimination has a marked effect on the immunomodulatory activity of

LL-37, the present study examined effects of citrullination on LL-37-dependent nucleic acid recognition by host cells. We found that citrullination has profound effects on the DNA-LL-37 interaction, resulting in significantly reduced activation of DCs and macrophages in response to bacterial DNA.

Materials and Methods

Reagents

Media components such as Gentamicin-Glutamine solution were purchased from Sigma (St. Louis, MO, USA). DMEM, Fetal Bovine Sera (FBS), Calcium- and Magnesium-Free PBS (without Ca^{2+} and Mg^{2+}), Penicillin-Streptomycin (PEST) and Lymphocyte Separation Medium were obtained from PAA (Germany). RPMI-1640 medium for human cell culture was from Gibco (NY, USA). Human blood for PBMCs isolation was obtained from Red Cross, Krakow, Poland. The Red Cross deidentified blood materials as appropriate for the confidentiality assurance of human subjects. Thus, this study adheres to appropriate exclusions from the approval of human subjects. CpG oligodeoxynucleotides (ODN 2216) with phosphorothioate (PS) backbone (5'-ggGGGACGA:TCGTCgggggg-3') were synthesized by Invivogen (San Diego, CA) and Biotinylated CpG (5'-BiotinGGGGGACGATCGTCGGGGGG-3') was synthesized by Genomed (Warsaw, Poland). A bacterial nucleotide sequence of 148 bp was amplified from *Tannerella forsynthia* genomic DNA. Native LL-37, scrambled peptide (sLL-37), LL-37 with arginine residues substituted by homoarginine (hArg-LL-37), different variants of the citrullinated peptide and variably carbamylated forms of LL-37 (Table I) were synthesized as per Koziel *et al.* (2014) (9) and Koro *et al.* (2016) (19). To eliminate a possibility of contamination of peptides with LPS, peptide solutions were tested using *Lymulus* Amebocyte Lysate (LAL) test, from Lonza, Germany.

In vitro citrullination of LL-37

The *in vitro* citrullination of LL-37 was performed according to the previously described protocol (9). Briefly, LL-37 was diluted to a concentration of 1 mg/ml in PAD assay buffer (100 mM Tris-HCl, 5 mM $CaCl_2$ and 5 mM dithiothreitol, pH 7.6) and incubated with either recombinant human PAD2 or PAD4 (Modiquest, Netherlands) at a concentration of 23 U/mg, for different time points (0, 15, 30, 120 min) at 37 °C. Citrullination was terminated by snap-freezing the samples.

Surface plasmon resonance

The interaction of native and modified LL-37 with DNA was determined using a Biacore 3000 instrument (Biacore). Selected DNA fragments, biotinylated at the 5′ end of the antisense strand (Bt-DNA) were immobilized on the SA sensor chip (GE Healthcare) with streptavidin covalently attached to the dextran. For the immobilization, the sensor surface was pre-treated according to the manufacturer's instruction and the solution of Bt-DNA (0.05 ng/μl) in 0.5 M NaCl was injected into the cell at a flow rate of 2 μl/min for 7 min. The chip surface was then washed with subsequent solutions of 0.5 M NaCl, 1 M NaCl and 0.1% SDS, for 3 min each at a flow rate of 20 μl/min, to remove non-specifically bound ligand. Further conditioning of the chip surface was performed with the running buffer (10 mM

Hepes, 150 mM NaCl, pH 7.4 with 0.05% P20 surfactant) until a stable baseline signal was obtained. The amounts of coupled DNA correspond to 210 response units (RU). A flow cell without DNA was used as reference. For the binding experiments a series of native and modified LL-37 peptide samples were prepared by dilution of 100 μM peptide stock solution in running buffer. The samples were injected over the sensor surface at 30 μl/min flow rate using 2 min interval for association and for dissociation process. The surface regeneration with 1 M NaCl for 30 sec was performed after each sample injection. Mass transfer effects did not influence the LL-37 binding. The analysis of the peptide mixtures was performed at the same conditions. The collected data were analysed using BIAevaluation software version 4.1 (Biacore).

Bacterial genomic DNA isolation and PCR Assay

T. forsythia genomic DNA, which was used as a template for our PCR assay, was isolated following the manufacturer's instructions (A&A Biotechnology, Poland). PCR was conducted using a 20 μl reaction mixture, which consisted of 20 ng of template DNA, 2 μl of *Taq* buffer KCl, 1.5 μl of 2 mM mixed dNTPs, 0.5 μl *Taq* DNA Polymerase and 10 μM of forward (5'-CTCGTAGTGTGCCTTCTTCCAC-3') and reverse (5'-GCCTGATCGGCATTCATTCGG-3') primers. PCR was performed with the following conditions: initial denaturation at 95 °C for 3 min, followed by 35 cycles of denaturation at 95 °C for 30 sec, annealing at 53 °C for 20 sec, extension at 72 °C for 30 sec and final extension at 72 °C for 5 min. This was followed with PCR purification as per the manufacturer instructions (Thermo Scientific, USA). The resultant PCR product was used to generate DNA-LL-37 complexes for a gel retardation assay.

Gel Retardation Assay

DNA-peptide complexes were generated as described by Chuang *et al.* 2009 (15). Bacterial genomic DNA was mixed with either synthetic native or modified forms of LL-37 or CRAMP at a 1:5 (DNA:peptide) molar ratio and incubated at room temperature for 10 min. The complex formation was determined with a gel retardation assay by running the complexes on 1.5 % agarose gel.

Spectra Analysis

The binding affinity between DNA with either native or PAD2/PAD4 citrullinated LL-37 was analysed by spectrophotometry. Complexes were first generated by incubation of DNA with the peptide at molar ratios of 1:0.5, 1:2, 1:10 (DNA:peptide) for 10 min at room temperature. The complexes were treated with diluted Quant-iT PicoGreen dye solution (1:200) according to manufacturer's instructions and the amount of unbound DNA was analysed across a spectrum of wavelengths 500 nm -600 nm with excitation at 485 nm.

Cell culture

pDCs were isolated from PBMCs with BD IMAG™ Cell Separation System (BD Biosciences). PBMCs were first separated from human peripheral blood by using density gradient centrifugation and pDCs were obtained following a manufacturer's protocol. pDCs were then seeded at 8×10^5 per well in 200 μl of complete medium (RPMI 1640 medium

supplemented with 10% FBS and 50 μg/ml Gentamicin). The cells were stimulated with either CpG alone or CpG together with differently citrullinated forms of LL-37. Both factors were mixed in PBS 10 min prior to cell stimulation at the indicated concentration: CpG (final concentration 3 μM) and LL-37 (final concentration 28.8 μg/ml) (molar ratio 1:1). Subsequently, cells were incubated with peptide-CpG mixtures for 15 min, washed with PBS 3 times and incubated in fresh complete medium overnight at 37 °C in a humidified 5% CO_2 atmosphere. Cell morphology was visualized by bright-field microscopy and images were taken, while culture supernatants were collected for cytokine measurement with ELISA.

RAW264.7 (0.2×10^6 cell/ml) were seeded in 200 μl of DMEM supplemented with 10% FBS and 50 μg/ml PEST overnight at 37 °C in a humidified 5% CO_2 atmosphere and adherent cells were washed with PBS once on the next day before fresh medium was added. Thereafter, macrophages were stimulated with CpG mixed with peptides as described above for pDCs.

Flow cytometry

pDCs (0.8×10^5 cells/mL) were incubated with a mixture of FITC-CpG (1.3 μg/ml) and different forms of LL-37 (6 μg/ml) for 15 min. Cells were washed three times with PBS and uptake of the complexes was determined by measuring the fluorescence intensity with flow cytometry (BD Biosciences). The mean fluorescence intensity and percentage of cells labeled with FITC-conjugated CpG were measured in each group. For phagocytosis inhibition, a 30 min preincubation step with cytochalasin D (5 μM) was introduced before adding the mixture of peptide with nucleic acid.

Cytokine measurement

The production of cytokines by RAW264.7 and pDCs was estimated with an ELISA kit. Cell culture supernatant was collected and the cytokine level of mouse TNF-α, human IL-6 (BD OptEIA™) and human IFN-α (PBL Interferon Source, NJ) were measured as per manufacturer's instructions.

DNAse Protection Assay

The assay was done as according to Lande *et al.* 2011 (28). To compare the efficiency of protection against DNase degradation between DNA-LL-37 and DNA-LL-37$_7$ complexes, 10 μg/ml of genomic DNA, which was isolated from HeLa cells as per the manufacturer's instructions (A&A Biotechnology, Poland), was incubated with 2 μM LL-37 and LL-37$_7$ respectively for 10 min at room temperature. The generated complexes were incubated with 100 U/ml DNase A (A&A Biotechnology, Poland) for 60 min at 37 °C, which was thereafter inactivated by incubating the samples at 75 °C for 10 min. The ability of such complexes to be protected from degradation was analysed with Quant-iT PicoGreen, excited at 480 nm with emission intensity recorded at 520 nm.

Identification of citrullinated forms of LL-37 in biological material

Attempts to identify the presence of deiminated LL-37 in serum, synovial fluid and NETs samples was carried out by Mass Spectrometry. Briefly, in order to identify the presence of LL-37, samples were either analyzed directly, separated by SDS-PAGE or ultra filtrated on a

10 kDa filter (Millipore), and LL-37 was collected in the filtrate. The region of the gel corresponding to LL-37 migration was in-gel digested (38). For whole sample or ultrafiltrate, the samples were lyophilized and denatured in 6 M Urea, 50 mM Tris-HCl, pH 8.0 and reduced and alkylated by sequential addition of 5 mM DTT and 15 mM iodoacetamide. After alkylation the samples were diluted 6 times to reduce the urea concentration and treated with Trypsin, Endoproteinase Glu-C (V8) or Endoproteinase Lys-C. The peptides were micro purified using C18 (Proxeon, Thermo Scientific).

Mass spectrometry

NanoESI-MS/MS analyses were performed on either an EASY-nLC II system (ThermoScientific) connected to a TripleTOF 5600 mass spectrometer (AB Sciex) or a NanoLC 415 (Eksigent) connected to a TripleTOF 6600 mass spectrometer (AB Sciex). The micro-purified peptides were dissolved in 0.1% formic acid, injected and trapped on an in-house packed trap column (2 cm × 100 μm I.D) with RP ReproSil-Pur C18-AQ 3 μm resin (Dr. Maisch GmbH). Peptides were eluted from the trap column and separated on a 15 cm analytical column (75 μm i.d.) packed in-house in a pulled emitter with RP ReproSil-Pur C18-AQ 3 μm resin (Dr. Maisch GmbH). Elution from the analytical column was performed with a linear gradient from 5% to 35% phase B (90% acetonitrile with 0.1% formic acid) over 20 min or 50 min. The collected MS files were converted to Mascot generic format (MGF) using the AB SCIEX MS Data Converter beta 1.1 (AB SCIEX) and the "proteinpilot MGF" parameters. The generated peak lists were searched against the swiss-prot database or a local database containing mature LL-37 using an in-house Mascot search engine (matrix science). Search parameters were adjusted to the applied protease and either propionamide (SDS-PAGE) or carbamidomethyl (iodoacetamide) was set as a fixed modification with peptide tolerance and MS/MS tolerance set to 10 ppm and 0.1 Da respectively.

Induction of NETs

Human blood was collected and PBMC and granulocyte-enriched fractions were harvested following LSM1077 (PAA Laboratories) gradient separation, as recommended by the manufacturer. The high-density fraction, containing neutrophils and erythrocytes, was mixed with a 1% solution of polyvinyl alcohol (Merck) in PBS and incubated for 20 min at room temperature. Neutrophils were harvested from the upper phase and subjected to hypotonic lysis to remove contaminating RBCs. After isolation, neutrophils were incubated for 30 min at 37 °C in humidified 5% CO_2 atmosphere, for cell adherence and were stimulated to induce NETs with 25 nM phorbol 12-myristate 13-acetate (PMA) for 3 h under the same incubation conditions. For PAD inhibition, 100 μM Cl-amidine (Calbiochem, USA) was applied (39). The release of NETs was quantified using PicoGreen dye (Invitrogen, OR). Samples were excited at 480 nm and the fluorescence emission intensity was measured at 520 nm using a spectrofluorometer.

Detection of LL-37 in NETs by immunofluorescence microscopy

NETs were prepared as described previously. Briefly, 1×10^5 cells were seeded on coverslips treated with syringe-filtered 1% BSA and incubated 30 min at 37 °C in humidified 5% CO_2 atmosphere. NET formation was stimulated with 25 nM PMA for 3 hours then fixed with 3.7% paraformaldehyde for 10 min at room temperature. After 3

washes with PBS, coverslips were incubated with mouse anti-human LL-37 (Hycult Biotech, Netherlands) (1:50 dilution factor) for 1 h at room temperature. After washing, samples were incubated with Alexa-Fluor-647 goat anti-mouse antibody (1:1000) (Jackson ImmunoResearch, USA) for 45 min at room temperature then counterstained with 1 μg/mL Hoechst 33342 (Invitrogen, USA) for 10 min at room temperature before being mounted to the slides and visualized with a fluorescence microscope at $20 \times$ magnification.

Quantification of human monocyte-derived macrophages (hMDMs) activation by NETs

Isolation of PBMCs was first performed from EDTA-treated human blood obtained from healthy donors (Red Cross, Krakow, Poland), using lymphocyte separation medium (PAA) density gradient system. The mononuclear cell fraction was collected and plated at $3 \times 10^6/$ well in 24-well plates (Sarstedt) with RPMI 1640 (PAA) supplemented with 2 mM L-glutamine, 50 μg/ml gentamicin (Sigma-Aldrich) and 10% autological human serum. After 24 h, non-adherent PBMCs were removed by washing with PBS and incubated with complete medium for 7 days to allow the differentiation of adherent cells to hMDMs. Medium was changed once every second day. Where indicated, hMDMs were primed with 100 ng/mL LPS for 4 h prior to stimulation. After washing with PBS, phenol-red free DMEM (PAA) was added to the primed cells and then they were treated for 2 h with NETs. Media were collected and quantification of IL-1β was done with commercially available ELISA as per manufacturer's instructions.

Western Blot

The protein concentration of NETs was determined by using the BCA protein assay (Thermo Scientific). Equal amount of proteins were mixed with loading buffer containing DTT and incubated for 5 min at 95 °C before separation on a 16% polyacrylamide gel. Materials on the gel were transferred to a methanol-activated polyvinylidene difluoride (PVDF) membrane for 180 min at 4 °C. Non-specific binding sites were blocked with 5% skimmed milk in TTBS buffer (20 mM Tris-HCL, 0.5 M NaCl, pH 7.5 with 0.05% Tween-20) for 4 h at room temperature before incubation with anti-human LL-37 monoclonal antibody (Hycult Biotech, Netherlands) diluted 1500-fold in TTBS buffer containing 3% BSA. Membranes were washed 3 times for 5 min with TTBS buffer and then incubated with anti-mouse IgG (1:20,000 dilution in TTBS buffer containing 3% BSA) for 2 h at room temperature. After washing with TTBS buffer (5 times for 5 min), the blots were developed using ECL detection (Western Blotting Detection Reagents; Amersham Biosciences, Chalfont St Giles, UK).

Derivatization of citrulline residues and detection of citrullinated proteins with anti-modified citrulline antibodies

NET samples standardized for equal protein amounts were first separated by SDS-PAGE prior transfer to PVDF membrane and the detection of citrullinated proteins was performed using an anti-citrulline (modified) detection kit (EMD Millipore, USA) according the manufacturer's protocol. Briefly, the membrane was blocked with 0.1% ovalbumin in TBS (1 M Tris, 3 M NaCl, pH 7.4) at room temperature for 15 min then citrulline residues were subjected to chemical modification at highly acidic pH. To this end, the membrane was incubated for 7 h at 37 °C with 1:1 solution composed of Mixture A (0.025% $FeCl_3$

solubilized in 98% H_2SO_4 and 85% H_3PO_4) and Mixture B (0.25% antipyrine, 0.5% 2,3-butanedione monoxime and 0.5 M acetic acid). After thorough rinses with water, the membrane was incubated for 30 min at room temperature in 3% skimmed milk in TBS (TBS-MLK) then overnight at 4 °C with antibodies specific for chemically modified citrulline (anti-AMC antibodies – Millipore) (1,000-fold diluted in TBS-MLK). After washing with water (2×), the membrane was incubated (with agitation) with 5,000-fold diluted goat anti-rabbit HRP conjugated IgG in TBS-MLK for 1 h at room temperature, washed again with water (2×) then with 0.05% Tween-20 diluted in TBS (2×, 5 min) and finally developed using ECL reaction.

Rhodamine-phenylglyoxal (Rh-PG) citrulline labelled probes

Citrullinated proteins in NETs were reacted with rhodamine-phenylglyoxal (Rh-PG), which chemoselectively labels citrulline over arginine at acidic pH as described by Bicker *et al.* 2012 (40). Hundred μl samples in 50 mM HEPES (pH 7.6) were treated with 20% Trichloroacetic acid (TCA) followed by 0.5 mM Rh-PG for 30 min at 37 °C. The reaction was quenched with 100 mM citrulline in HEPES (pH 7.6) for 30 min at 37 °C. The samples were placed on ice for 30 min after the incubation to facilitate protein precipitation with TCA. Next, samples were centrifuged at $16,000 \times g$ for 15 min at 4 °C. Supernatant was discarded and 250 μl of ice-cold acetone was added without disturbing the pellet. Samples were then centrifuged again at $16,000 \times g$ for 10 min at 4 °C. The supernatant was discarded and tubes were left to dry for 10 min to vaporize residual acetone. To quench the residual probe, 20 μl of 100 mM arginine in HEPES (pH 7.6) were added followed by interval sonication for 2×5 sec and then samples were incubated at 95 °C for 5 min before storage at −20 °C. The samples were run on 16% polyacrylamide gel at 120 V and fluorescent bands were visualized using Bio-Rad Gel Imager with a Rhodamine filter (560/50).

The estimation of LL-37 half-life in biological fluids

To determine the stability of citrullinated forms of LL-37 in different environments, the peptides were added to NETs, inflamed (from RA patients) and control (from healthy individuals) human sera, as well as to synovial fluid obtained from rheumatoid arthritis patients. Briefly, all biological samples were centrifuged at 13,000 rpm for 15 min to remove lipids and precipitated material. Supernatants (900 μl) were mixed with 100 μl peptide solutions (1 mg/ml solution in PBS). Peptides mixed with PBS were used as a control. Samples were incubated at 37 °C and at different time points aliquots (50 μl) were withdrawn and treated with 50 μl of 6 M urea and 50 μl 6% TFA to denature all proteins in a sample. Next, samples were centrifuged at 13,000 rpm, 15 min and peptides in supernatants were separated by UPLC Nexera (Shimadzu Japan) on the C8 analytical column (Aeris) equilibrated with 0.1 TFA in water at flow rate 0.4 ml/min. Peptides were eluted with acetonitrile gradient up to 55% developed in 12 min. Proteinaceous material eluted from the column was detected at 208 nm.

pDCs stimulation with NETs

pDCs were seeded at a density 0.8×10^5 per well before being stimulated overnight at 1:3 dilution with NETs, together with, or without, anti-LL37 antibodies (Hycult Biotech, mAb 1-1C12, Netherlands), 5 μM native LL-37 or hArg-LL-37. After an overnight incubation, the

supernatant of pDCs was collected and quantification of hIL-6 was done with a commercially available ELISA. The isolation of RNA was performed using the TRIzol method as described elsewhere. Seven hundred ng of total RNA was reverse-transcribed using a High Capacity cDNA Reverse Transcription kit (Applied Biosystems, Carlsbad, CA) as per the manufacturer's instructions. Following synthesis, cDNA was subjected to quantitative real-time PCR analysis using the Bio-Rad CFX96 Real-Time PCR Detection System (Bio-Rad, Hercules, CA, USA) and Sybr Green-based JumpStart™ Taq ReadyMix™ (Sigma Aldrich, USA). The relative expression of *MXA* (5′-ACTCTGTCCAGCCCCGTAGAC-3′ (Forward); 5′ TCACAGCTTCCTGCTAAATCACC-3′ (Reverse)) was normalized to the expression of *EF2* (5'-GACATCACCAAGGGTGTGCAG-3' (Forward); 5′-TTCAGCACACTGGCATAGAGGC-3′ (Reverse)) in the same sample. After the denaturation step (5 min at 95 °C), conditions for cycling were: 39 cycles of 30 s at 95 °C, 30 s at 56 °C and 45 s at 72 °C. The fluorescence signal was measured after the extension step at 72 °C and a melting curve was generated to verify the specificity of the PCR product after the end of the PCR cycling. All samples were run in triplicates.

Statistical Analysis

All experiments were performed at least in triplicate and the results were analyzed for statistical significance using unpaired Student's *t* tests and ANOVA. All values are expressed as means ± SD and differences were considered significant when p < 0.05. Statistical analysis was performed using GraphPad Prism 7.0.

Ethical statement

The studies using human probes of serum and synovial fluid were performed according to the agreement of the Committee of Ethics at the University of Bergen (nr. 242.06).

Results

Enzymatic citrullination of LL-37 by human PADs regulates formation of DNA/LL-37 complexes

LL-37 binds nucleic acids to form aggregated and condensed structures, thereby protecting DNA from degradation (10, 15). However, LL-37 released into the inflammatory milieu together with PADs may be deiminated, which modifies the function of the peptide (6,9). Therefore, we asked whether citrullination affects the affinity of LL-37 for DNA. We found that the ability of LL-37 to form complexes with DNA was dose-dependent, with the most efficient binding occurring at a molar ratio of 1:10 (DNA:LL-37) (Figure 1A). Next, to assess how citrullination affects the affinity of LL-37 for DNA, we incubated LL-37 with recombinant PAD2 or PAD4 for different times (15 to 120 min). Citrullination reduced the affinity of LL-37 for DNA in a time-dependent manner. The effect was already visible after 15 min, and increased gradually over time (Figure 1B, C, and D). Although both PAD2 and PAD4 inhibited the interaction between LL-37 and DNA, PAD2 was more effective; indeed, PAD4 required double the time to achieve a similar end point (Figure 1D). As a control we analyzed the DNA binding by scrambled LL-37 (sLL37) and its citrullinated version obtained by incubation with PAD2, and found that none of them bound to nucleic acids

(Figure 1E). Additionally, we verified the role of Arg guanidinium side chains in DNA binding using LL-37 with Arg residues substituted by homoarginines (hArg-LL-37), which are insensitive to enzymatic deimination (data not shown). The analysis revealed that hArg-LL-37 bound DNA with the efficiency equivalent to that of native LL-37 and, as expected, preincubation of the peptide with PAD2 had no influence on this interaction (Figure 1F).

Inflammation is associated with excessive post-translational modifications of proteins and peptides, which often alters their function (17). One such modification is carbamylation, a chemical reaction that converts lysine into homocitrulline. This reaction occurs *in vivo* during inflammation; patients with RA generate antibodies to carbamylated proteins (18). LL-37, which contains six lysine residues, is particularly susceptible to carbamylation, and these modifications alter the cationic and amphipathic nature of the peptide (19). Therefore, we examined whether formation of complexes between LL-37 and DNA are affected by peptide carbamylation. We tested several synthetic forms of carbamylated LL-37 (Table I) and found that, in stark contrast to citrullination, carbamylated peptides had affinity for DNA comparable to that of native LL-37 (Figure 1G). Importantly, enzymatic deimination of Arg residues in carbamylated LL-37 totally abolished their ability to bind nucleic acids (Figure 1H).

Taken together, we documented that the guanidinium side chains of Arg (or hArg) residues in the context of the LL-37 sequence are essential for DNA binding since their modification at defined positions, but not peptide cationicity alone, interferes with the LL-37 interaction with DNA.

Characterization of DNA:citrullinated LL-37 complex formation

We next examined effect of LL-37 citrullination on DNA binding in more detail by using surface plasmon resonance (SPR) to analyze the interaction between DNA and synthetic forms of LL-37 harboring different numbers of citrulline residues (Arg^7Cit ($LL-37_7$), $Arg^{7,29}Cit$ ($LL-37_{7,29}$), $Arg^{7,29,34}Cit$ ($LL-37_{7,29,34}$, and $Arg^{7,19,23,29,34}Cit$ ($LL-37_{all\ cit}$; Table I). We found that the strength of binding to DNA fell to background levels as the level of citrullination increased (Figure 2A). We found it interesting that just a single substitution (Arg to Cit) at position 7 in LL-37 led to a marked (3-fold) reduction in the affinity of the peptide for DNA (Figure 2A). The results were confirmed in a gel-retardation assay (Figure S1A). Moreover, when compared with DNA complexed to the native peptide, DNA associated with the modified peptide was more susceptible to degradation by DNAse (70.18% intact *vs.*, 35.45% intact. respectively) (Figure 2B). Taken together, these data argue that $LL-37_7$ binds DNA less tightly and that the complex may have a more relaxed structure than that of native LL-37.

Citrullination of LL-37 by PAD2 and PAD4 generates a spectrum of variably citrullinated peptides (9). Therefore, we tested mixtures of synthetic modified forms of LL-37, the composition of which resembles the final products generated by PAD2 (mPAD2) and PAD4 (mPAD4) (Figure S1B) (9). Analysis of both mixtures (mPAD2 and mPAD4) by SPR excluded any interaction between the peptides themselves, since DNA binding by the peptides in the mixture clearly resembled the additive binding effects of the individual

peptides (Figure S1C, D). Taken together, these results suggest that deimination of particular arginine residues within LL-37 does not affect peptide interactions.

To examine the generality of the effects of citrullination on formation of DNA-peptide complexes, we next tested native and deiminated variants of murine cathelicidin, CRAMP (Table I). The results of a retardation assay confirmed that CRAMP formed complexes with bacterial DNA (16), and that citrullination of a single Arg residue in CRAMP inhibited complex formation (Figure 2C). This finding indicates that deimination of cathelicidin hinders its ability to form a complex with DNA, and that this effect is not species-specific. Furthermore, modification of even a single Arg residue within the bactericidal peptide had a significant effect on its interaction with nucleic acid.

Effect of LL-37 citrullination on activation of pDCs and macrophages by CpG

By acting as a carrier molecule that facilitates internalization of bacterial or self-DNA molecules into the endosomal compartment of pDCs, LL-37 increases the immunogenic potential of DNA (10). LL-37 complexed with DNA fragments stimulates pDCs to produce much larger amounts of IFN-α than cells exposed to DNA alone (10). Together with our own results, these findings prompted us to assess how citrullination affects LL-37-dependent DNA-mediated activation of myeloid cells. Using synthetic oligonucleotides resembling bacterial DNA (CpG), we showed that exposing pDCs to CpG complexed with native LL-37 caused cells to clump, a feature characteristic of pDCs activation. The degree of cell clumping displayed an inverse relationship with the level of peptide citrullination, and was much less pronounced in cells treated with CpG alone or with a mixture of CpG and fully-citrullinated LL-37 (Figure 3A).

This qualitative difference was unambiguously confirmed by an assay measuring the amount of secreted IFN-α. While neither the peptide nor CpG alone stimulated secretion of IFN-α, a complex of CpG with the native peptide had a strong effect (Figure 3B). The effect was significantly weaker when CpG was complexed with LL-37$_7$ or LL-37$_{7,29,34}$, or (most notably) fully-citrullinated LL-37, which led to an ~10-fold reduction in IFN-α secretion (Figure 3B). Importantly, changes in IFN-α secretion showed a negative association with IL-6 levels measured in conditioned medium (Figure 3C), which were elevated only in cells exposed to CpG alone or a mixture of CpG and the fully-citrullinated peptide.

Given that activation of pDCs by CpG-LL-37 is dependent on internalization of the complex (10), we next measured the degree of complex formation within cells. For these experiments, we treated cells with native LL-37 complexed with FITC-labeled CpG. We found that pDC-associated fluorescence was readily detectable by flow cytometry. By contrast, binding between cells and complexes containing citrullinated peptides was reduced in line with level of peptide modification, reaching background levels in the case of fully-citrullinated LL-37 (Figure S2A). This may be due to hindered CpG deposition on the cell membrane, since uptake of FITC-labeled CpG by phagocytic pDCs in the presence or absence of cytochalasin D (an inhibitor of phagocytosis) showed the same staining profile (Figure S2B). These findings suggest that impairment of pDC activation by nucleic acid in the presence of citrullinated peptides is caused by reduced affinity of the complex for the pDC membrane, which affects delivery of DNA into the intracellular/endosomal compartment.

Given that murine macrophages express TLR-9, and that macrophages are activated by CpG (20), we next investigated the effect of CpG complexed with native and citrullinated LL-37 on macrophage activation (21). As for pDCs, RAW264.7 cells were activated by DNA complexed with the native peptide, as manifested by secretion of high amounts of TNF-α (Figure 3D). Also, the complex containing LL-37$_7$ had a strong stimulatory effect. By contrast, highly-citrullinated forms of LL-37 (LL-37$_{7,29,34}$ and LL-37$_{all\ cit}$) complexed with CpG elicited significantly weaker effects on macrophages (Figure 3D). A similar effect was observed after treatment of macrophages with murine cathelicidin (the CRAMP peptide) complexed with DNA. Whereas native CRAMP/CpG activated macrophages, the CRAMP variant harboring a single arginine replaced by citrulline lacked this ability (Figure 3D [insert]).

The analyses using a scrambled peptide, which cannot bind to DNA, revealed that sLL-37 was unable to sensitize macrophages to recognize nucleic acid. In contrast LL-37 with homoarginines (hArg-LL-37) exerted similar effect to the native peptide, when complexed with CpG (Figure 3D). Most strikingly, however, the carbamylated variants of LL-37, despite remarkably decreased cationic character (19), preserved the full immunostimulatory potential of the native peptide with respect to DNA recognition by macrophages (Figure 3D). The same was found using dendritic cells (data not shown).

Finally, to mimic physiological conditions, we examined activation of RAW264.7 cells by DNA in the presence of a mixture of different forms of LL-37 generated by incubating the peptide with PADs (Figure S1B). As shown in Figure 3E, pre-treating LL-37 with PAD-2 and PAD-4 led to a significant reduction in the ability of the peptide to stimulate TNF-α production in conjunction with DNA.

Cumulatively these results unbiasedly argue that not just a change in the positive charge of the peptide but the deimination of arginine residues in the context of the native LL-37 sequence strongly and specifically affects the proinflammatory function of LL-37 as the inducer of the response of APCs to extracellular DNA.

Identification of citrullinated LL-37

PADs are released into inflammatory exudates and their extracellular activity is associated with citrullination of many proteins in the extracellular matrix and blood plasma (9). The high efficacy of PADs to deiminate Arg residues within LL-37 *in vitro* suggests that this modification also occurs *in vivo*, particularly at sites of infection/inflammation at which the peptide acts as a substrate for citrullination. Nevertheless, no study has yet demonstrated the presence of citrullinated LL-37 in pathophysiological fluids. To address this, we examined tissues from healthy controls and patients with inflammatory conditions. We also examined NET structures, sites where both substrate (LL-37) and active PAD enzymes co-exist at relatively high concentrations (22).

First, we performed Western blot analysis to see whether modified peptides are recognized by antibodies developed against native LL-37. In contrast to native LL-37, no band was seen when synthetic, fully-citrullinated LL-37 (LL-37$_{all\ cit}$) was incubated with the anti-LL37 antibody (Figure 4A). These data suggest that citrullination of LL-37 destroys an epitope(s)

recognized by the LL-37 antibody, simultaneously generating epitopes that react with anti-AMC antibodies that are specific for citrulline residues (Figure 4A). Subsequent Western blot analysis using differentially-citrullinated synthetic LL-37 peptides revealed that binding of anti-LL37 antibody decreased as the number of citrullinated arginine residues in LL-37 increased. Figure 4B shows that amount of LL-37$_7$ and LL-37$_{7,29}$ recognized by the antibody was less than the amount of non-citrullinated peptide, and that binding was absent when LL-37 contained more than two citrullinated arginine residues. We observed the same effect in an ELISA assay (data not shown). Taken together, these data explain why assays based on antibodies specific for native LL-37 failed to detect some modified forms of LL-37.

Next, we used rhodamine-phenylglyoxal (Rh-PG), a chemical probe that reacts specifically and covalently with citrulline residues in proteins and peptides. Fluorescent imaging of NETs generated from human neutrophils treated with PMA and resolved by SDS-PAGE revealed a faint band at the same level as exogenous citrullinated LL-37 added to NETs (Figure S3). The intensity of the band was reduced in the presence of a PAD inhibitor (chloramidine/Cl-amidine/Cl-A), suggesting peptide modification. To confirm the presence of LL-37 in rhodamine-phenylglyoxal-labeled samples, the bands corresponding to untreated NETs were in-gel digested with trypsin and analyzed by MS. The probes revealed the presence of a mature LL-37 N-terminus; however, no other LL-37-derived peptides were identified (Figure 4C). We confirmed the presence of LL-37 in NETs using a targeted MS/MS analysis approach. Media containing NETs was ultra-filtrated and treated with the LysC endopeptidase. LysC generated N- and C-terminal peptides that were detectable by MS (Figure S4). The N-terminal peptide LLGDFFRK was also evidence of mature LL-37, since the C-terminal peptide is produced by cleavage at the …FA#LL…, peptide bond, which is not cleaved by LysC. Both peptides were identified in NET-containing medium, confirming the presence of mature LL-37. However, neither of the peptides was identified in a citrullinated form. Several different methods were used to prepare samples, including in-gel digestion, precipitation, ultrafiltration, and various combinations thereof; all were unsuccessful in identifying citrullinated LL-37. The N- and C-terminal unmodified peptides in LysC digested NETs were present only at the limit of detection; in addition, the fragmentation pattern of citrullinated synthetic peptides is very complex due to a high level of internal fragmentation and neutral loss (23). The combination of low ion intensity, a noisy fragmentation pattern, and a heterogeneous modification pattern meant that modified LL-37 peptides were below the limit of detection. Furthermore, the inability to identify modified LL-37 may be due to the short lifespan of citrullinated peptides. Therefore, we examined the stability of synthetic citrullinated forms of LL-37 in sera from healthy donors, sera and synovial fluid from RA patients, as well as in NET samples. Figure 4D shows that the half-life of LL-37 was comparable with that of LL-37$_7$, but was shorter for peptides with higher levels of citrullination (LL-37$_{7,29,34}$ and LL-37$_{all\ cit}$); this was most marked in synovial fluid from RA patients. The tested modified LL-37 peptides showed highest stability in healthy serum, but were rapidly degraded in NETs and in synovial fluid from RA patients (Figure 4D), what may explain the identification issues.

Finally, we tried to identify deiminated LL-37 in PMA-induced NETs in which the structures of the DNA filaments coated with antimicrobial components such as elastase or

LL-37 are visible upon immunofluorescence staining (24). Of note, NET formation depends strongly on the activity of PAD-4 (25). Again, we used the PAD inhibitor Cl-A, which reduced both the levels of citrullination (Figure S3) and NET formation (Figure 5A, C). Immunofluorescence analysis using antibodies specific for native LL-37 showed that NETs generated in the presence of Cl-A contained more LL-37 than those generated in the absence of the inhibitor (Figure 5B, C). The calculation of the ratio between LL-37 positive staining and amount of NETs revealed that in comparison to samples prepared in the absence of the inhibitor, NETs generated by PMA in the presence of Cl-A contained 3 times more LL-37 fluorescence spots (Figure 5C – insert). This observation was further confirmed when we estimate the degree of NET generation in the presence of anti-LL-37 antibodies. As reported by Lande *et al.* 2011, anti-LL-37 antibodies increased NETosis upon specific binding to LL-37 released by neutrophils isolated from patients suffering from SLE. However, we could not replicate this observation using neutrophils from healthy donors in the PMA-induced NETs model. Significantly, however, the effect was visible when neutrophils were exposed to Cl-A (Figure 5D). This indicates that a higher amount of native LL-37 was present in Cl-A-treated neutrophils, in keeping with our observation that anti-LL-37 can only recognize the native form of the peptide. As the monoclonal antibody recognizes both proteolytically processed LL-37 and its precursor form, hCAP18, we performed immunoblot analysis of PMA-induced NETs. Our results revealed that the propeptide is externalized during NETosis induced by PMA or *S. aureus*. Moreover, compared with samples not exposed to the inhibitor, far more hCAP18 (visible at 18 kDa) was found in neutrophils pre-treated with Cl-A (Figure 5E), which may suggest LL-37 precursor citrullination during NET formation. This trend was also observed for the mature peptide (4.7 kDa) in NETs induced by both PMA and *S. aureus* (Figure 5E). Taken together, the effect of Cl-A on the amount of hCAP18 detected in NETs argues strongly that both cathelicidin and mature LL-37 are citrullinated by PADs during NET formation, both *in vitro* and *ex vivo*.

The final indirect evidence for the presence of citrullinated LL-37 within NETs was obtained using a model described by Kahlenberg *et al.* 2012 (26), in which human monocyte-derived macrophages are primed with LPS to increase surface expression of the P2X7 receptor, which recognizes cathelicidin. Primed macrophages release high levels of IL-1β upon stimulation with LL-37. Therefore, we used this model system to determine the presence of stimulatory LL-37 in NETs. First, we showed that citrullination of LL-37 strongly abrogated inflammasome activation in a manner dependent on the degree of modification. Then, we showed that even a relatively short exposure of LL-37 to human PADs led to a significant reduction in the ability of the peptides to stimulate release of IL-1β from LPS-primed macrophages (Figure 5F). Finally, we found that NETs pre-treated with Cl-A had a much stronger effect on primed macrophages, as shown by IL-1β secretion, than native NETs (Figure 5G). This argues unambiguously that during NETosis, LL-37 is released from hCAP18 and, at least partially, simultaneously citrullinated as the treatment with Cl-A prevented extensive modification of the peptide. Furthermore, these data suggest that *in vivo* citrullination of LL-37 within NETs plays an important immunomodulatory role.

Effect of citrullination on immunomodulation regulated by NETs

To further explore the immunomodulatory potential of LL-37 citrullination in the context of acquired immunity, we examined the effect of NETs on pDC activation. Stimulation of pDCs with PMA-induced NETs resulted in formation of cell clumps, a morphological change characteristic of pDC activation. Cell clumping was enhanced when NETs were collected from neutrophils treated with Cl-A before (Cl-A/PMA) or 2 hours post-incubation with PMA (PMA/Cl-A) (Figure 6A). To shed light on the molecular mechanism underpinning changes in pDC physiology/phenotype, we performed transcriptome analysis of genes regulated by IFN-α. We found that expression of *MxA* fell upon exposure of pDCs to NETs/PMA, but was upregulated markedly by exposure to NETs pre-treated with Cl-A (Cl-PMA) (Figure 6B). Of note, MxA plays an antiviral role in that it is an important effector protein in the type I IFN response (27). Furthermore, while secretion of IL-6, another marker typical of pDC activation, was increased only slightly upon exposure of pDCs to NETs/PMA, a substantial amount of IL-6 was found in conditioned medium from pDCs treated with NETs generated in the presence of Cl-A (Figure 6C). Finally, we analyzed if supplementation of NETs with native LL-37 or hArg-LL-37 will influence the inflammatory potential of those structures towards pDCs. Our data revealed that, in contrast to the native peptide, addition of hArg-LL-37, which is not citrullinated by the PADs, significantly increased the inflammatory response of phagocytes (Figure 6D, E).

Taken together, these data suggest that pDCs showed increased activation in response to NETs containing smaller amounts of citrullinated protein (due to PAD inhibitor treatment of PMA-activated neutrophils). Thus, we postulate that LL-37 and its citrullination are factors that may affect the inflammatory potential of NETs.

Discussion

Recognition of bacterial genomic DNA by intracellular TLR9 receptors triggers immune responses and promotes production of inflammatory cytokines. This signaling pathway is enhanced by LL-37, which binds nucleic acids with high affinity and facilitates DNA uptake into the endosomal compartments of APCs. This action of LL-37 is partly explained by the increased affinity of the DNA-peptide complex for the host cell membrane, and by arrest of the internalized complex in the early endosome, which increases production of IFNs. In the event of bacterial infection, this pathway is beneficial since it increases the immune response. However, there is a downside. The release of large amounts of DNA from dying host cells during an inflammatory response may lead to an overwhelming proinflammatory response, as observed in patients with psoriasis and SLE (28).

Recent findings show that inflammation is strongly regulated by post-translational modification of immunomodulators, including LL-37. In this context, we focused on citrullination of proteins and peptides, a process catalyzed by the calcium-dependent PADs, which are present at inflammatory foci. LL-37 is highly susceptible to citrullination by human PAD2 and PAD4 as it contains five Arg residues (6,9). Deimination of the peptide changes its primary function, including its antibacterial and chemotactic activity (6) and abrogates its anti-inflammatory potency as an antagonist of TLR-dependent signaling induced by LPS, LTA, and PGN (9). Here, we focused on the role of LL-37 in cell signaling

mediated by nucleic acids. First, we show that citrullination of LL-37 has a marked effect on its affinity for nucleic acids. *In vivo*, citrullination in the inflammatory milieu would be performed predominantly by phagocyte-derived PAD2 and PAD4, with the former being more efficient (Figure 1B–D and Koziel et al., 2014). Next, we examined the effect of citrullination on regulation of the LL-37-dependent immune response to CpG motifs. Using different forms of synthetic citrullinated LL-37 peptide, we showed that deimination inhibits cell activation, as manifested by a fall in the amount of proinflammatory cytokines as the number of citrullinated arginine residues present in the peptide increased. The weakened affinity of deiminated LL-37 for DNA reduces complex formation and subsequent binding to the cell membrane. This in turn results in less CpG entering the endosomal compartment of pDCs, thereby abrogating IFN-α production and desensitizing the cells to DNA.

The half-life of DNA in the inflammatory milieu is regulated by the action of DNases released by dying cells (29). However, formation of complexes containing LL-37 protects DNA from degradation and allows successful uptake of nucleic acids by surrounding cells, including immune cells, and their subsequent transport to the nuclear compartment (30). To this end, we showed that citrullination hinders the interaction between LL-37 and nucleic acids, making the latter more susceptible to degradation by DNAse (Figure 2B) and reducing their proinflammatory potential. Taken together, our results suggest that citrullination of LL-37 leads to a significant down-regulation of the host response to cell-free DNA. Remarkably, the effect was not entirely related to the reduced cationic character of LL-37, rather, it appears to be highly specific to arginine modification. Such a conclusion arises from the observation that carbamylation of lysine residues in the peptide did not affect peptide binding to DNA or activation of myeloid cells (Figure 1G, 3D). Together with the findings that hArg-LL-37 elicits similar activity to native LL-37 (Figure 1F) and the carbamylated forms of LL-37 upon enzymatic deimination lose the DNA-binding binding ability (Figure 1G, H) irrefutably argues that Arg residues in LL-37 are essential for the LL-37 interaction with DNA and stimulation of antigen presenting cells. This is in keeping with the unique role of the guanidinium side chain of Arg residues in protein or peptides interaction with ribonucleic acids (41).

NETosis is a convenient model for studying the effect of LL-37 citrullination on its interaction with DNA since the interaction between DNA and LL-37 in NETs is well described (24, 28). LL-37 as an integral component of NETs and has pluripotent biological functions. In addition to antibacterial activity against entrapped pathogens, LL-37 protects NETs against degradation by bacterial nucleases (31). Moreover, the presence of LL-37 in NETs activates the inflammasome in macrophages (26). Perplexingly, however, no attention is paid to the fact that the abundance of LL-37 in NETs means that it is exposed to PAD activity (22), which might catalyze citrullination of the peptide. Therefore, we tried to identify modified forms of LL-37 in NETs. Experiments using antibodies recognizing only the native form of the peptide revealed that NETs generated in the presence of a PAD inhibitor contained more unmodified LL-37 than control NETs (Figure 5). This supports (indirectly) citrullination of the peptide. Unfortunately, our attempts to identify citrullinated forms of LL-37 in NETs directly by mass spectrometry analysis failed. This might be due to degradation of citrullinated LL-37 by neutrophil proteases that are also abundant in NETs. Such a conclusion is strongly supported by our finding that citrullinated LL-37 has a

significantly shorter half-life than the native peptide in NETs and synovial fluid from RA patients (Figure 4). Of note, the latter is known to contain NETs (32). Furthermore, the oxidative environment resulting from myeloperoxidase activity can lead to additional modification of both citrulline and other residues in LL-37 (33). Any additional modifications will prevent identification by mass spectrometry due to a mass shift (34). Interestingly, all LL-37 variants were stable in serum samples, in keeping with lack of any significant proteolytic activity in this fluid; this suggests proteolytic degradation as the reason for the short life-time of citrullinated LL-37 in NETs. Indeed, treatment of NETs with a protease inhibitor cocktail before the peptides were added prevented their degradation and ameliorated differences in the half-life (data not shown). Our data support the rapid degradation of citrullinated peptides reported by Klisgard *et al.* 2012 (6). Taken together, we postulate that citrullinated LL-37 is generated during NET formation.

Several studies report crosstalk between NETs and DCs (24, 28, 35), and it is postulated that LL-37-DNA complexes contribute to excessive activation of pDCs and underpins the pathogenesis of autoimmune diseases such as SLE and psoriasis. Therefore, we used NETs to confirm the pathophysiologically relevant role of LL-37 citrullination during modulation of myeloid cell responses to nucleic acids. Myeloid cells exposed to NETs generated in the presence of a PAD inhibitor were activated to a greater extent than when exposed to native NETs. The increased proinflammatory effect exerted by native proteins in NETs strongly suggests that citrullination of LL-37 makes a marked contribution to regulating the DNA response of myeloid cells exposed to NETs, including pDCs and macrophages. Our conclusion is strongly supported, since LL-37 with homoarginines (hArg-LL-37), which are not deiminated by the PADs, significantly enhanced the proinflammatory potential of NETs towards dendritic cells. Therefore, we hypothesize that control and/or restriction of the inflammatory potential of NETs is executed at the level of post-translation modification of proteins associated with DNA fibers. Moreover, one may propose that the activity and stability of proteins bound to the DNA meshwork is strictly and dynamically regulated by the host to eliminate pathogens without unwanted side effects (e.g., excessive inflammation).

Taken together, the results presented herein show that citrullination of LL-37 plays a critical role in the host responses to cell-free DNA. Inhibition of the interaction between DNA and citrullinated LL-37, or enhanced degradation of the modified peptide, dampens activation of myeloid cells by nucleic acids. This may be a disadvantage during bacterial infection; however, it may be an important mechanism that protects the host against overactivation of the immune system and development of autoimmune diseases, especially those in which an overwhelming response to self-DNA molecules is crucial (i.e., RA, psoriasis, chronic obstructive pulmonary disease, psoriasis) (36, 37). Therefore, the advent of PAD inhibitors designed to treat RA and other diseases means that it is important to monitor and quantify levels of modified LL-37 *in vivo*, and to verify (*in vivo*) the role of peptide citrullination in health and disease.

Supplementary Material

Refer to Web version on PubMed Central for supplementary material.

Acknowledgments

Abbreviations

LL-37	cathelicidin
PAD	peptidyl arginine deiminase
pDCs	plasmacytoid dendritic cells
NETs	neutrophil extracellular traps

References

1. Sørensen OE, Follin P, Johnsen AH, Calafat J, Tjabringa GS, Hiemstra PS, Borregaard N. Human Cathelicidin, hCAP-18, is processed to the antimicrobial peptide LL-37 by extracellular cleavage with proteinase 3. Blood. 2001; 97(12):3951–3959. [PubMed: 11389039]

2. Niyonsaba F, Iwabuchi K, Someya A, Hirata M, Matsuda H, Ogawa H, Nagaoka I. A cathelicidin family of human antibacterial peptide LL-37 induces mast cell chemotaxis. Immunology. 2002; 106(1):20–26. [PubMed: 11972628]

3. Zasloff M. Antimicrobial peptides of multicellular organisms. Nature. 2002; 415:389–395. [PubMed: 11807545]

4. Nagaoka I, Hirota S, Niyonsaba F, Hirata M, Adachi Y, Tamura H, Tanaka S, Heumann D. Augmentation of the lipopolysaccharide-neutralizing activities of human cathelicidin CAP18/ LL-37-derived antimicrobial peptides by replacement with hydrophobic and cationic amino acid residues. Clin Diagn Lab Immunol. 2002; 9(5):972–982. [PubMed: 12204946]

5. Ramos R, Silva JP, Rodrigues AC, Costa R, Guardão L, Schmitt F, Soares R, Vilanova M, Domingues L, Gama M. Wound healing activity of the human antimicrobial peptide LL37. Peptides. 2011; 32(7):1469–1476. [PubMed: 21693141]

6. Kilsgård O, Andersson P, Malmsten M, Nordin SL, Linge HM, Eliasson M, Sörenson E, Erjefält JS, Bylund J, Olin AI, Sørensen OE, Egesten A. Peptidylarginine deiminases present in the airways during tobacco smoking and inflammation can citrullinate the host defense peptide LL-37, resulting in altered activities. Am J Respir Cell Mol Biol. 2012; 46:240–248. [PubMed: 21960546]

7. Mohanan S, Cherrington BD, Horibata S, McElwee JL, Thompson PR, Coonrod SA. Potential role of peptidylarginine deiminase enzymes and protein citrullination in cancer pathogenesis. Biochemistry Research International. 2012; 2012:11. Article ID 895343.

8. Hensen SMM, Pruijn GJM. Methods for the detection of peptidylarginine deiminase (PAD) activity and protein citrullination. Mol Cell Proteomics. 2014; 13(2):388–396. [PubMed: 24298040]

9. Koziel J, Bryzek D, Sroka A, Maresz K, Glowczyk I, Bielecka E, Kantyka T, Pyr K, Svoboda P, Pohl J, Potempa J. Citrullination alters immunomodulatory function of LL-37 essential for prevention of endotoxin-induced sepsis. The Journal of Immunology. 2014; 192:5363–5372. [PubMed: 24771854]

10. Lande R, Gregorio J, Facchinetti V, Chatterjee B, Wang YH, Homey B, Cao W, Wang YH, Su B, Nestle FO, Zal T, Mellman I, Schröder JM, Liu YJ, Gillet M. Plasmacytoid dendritic cells sense self-DNA coupled with antimicrobial peptide. Nature. 2007; 449(7162):564–569. [PubMed: 17873860]

11. Hurtado P, Chen AP. LL-37 promotes rapid sensing of CpG oligodeoxynucleotides by B lymphocytes and Plasmacytoid dendritic cells. Journal of immunology. 2010; 184:1425–1435.

12. Conrad C, Meller S, Gilliet M. Plasmacytoid dendritic cells in the skin: to sense or not to sense nucleic acids. Seminars in immunology. 2009; 21:101–109. [PubMed: 19250840]

13. Zhang X, Oglecka K, Sandgren S, Belting M, Esbjörner EK. Dual functions of the human antimicrobial peptide LL-37-target membrane perturbation and host cell cargo delivery. Biochim Biophys Acta. 2010; 1798:2201–2208. [PubMed: 20036634]

14. Kaplan MJ, Radic M. Neutrophil extracellular traps (NETs): Double-edged swords of innate immunity. Journal of Immunology. 2012; 189(6):2689–2695.

15. Chuang CM, Monie A, Wu A, Mao C-P, Hung C-F. Treatment with LL-37 peptide enhances anti-tumour effects induced by CpG oligodeoxynucleotides against ovarian cancer. Human Gene Therapy. 2009; 20:303–313. [PubMed: 19272013]

16. Döring Y, Manthey HD, Drechsler M, Lievens D, Megens RT, Soehnlein O, Busch M, Manca M, Koenen RR, Pelisek J, Daemen MJ, Lutgens E, Zenke M, Binder CJ, Weber C, Zernecke A. Auto-antigenic protein-DNA complexes stimulate plasmacytoid dendritic cells to promote atherosclerosis. Circulation. 2012; 125(13):1673–1683. [PubMed: 22388324]

17. Valesini G, Gerardi MC, Iannuccelli C, Pacucci VA, Pendolino M, Shoenfeld Y. Citrullination and autoimmunity. Autoimmunity reviews. 2015; 14(6):490–497. [PubMed: 25636595]

18. Pruijn GJM. Citrullination and carbamylation in the pathophysiology of rheumatoid arthritis. Frontiers in Immunology. 2015; 6:192. [PubMed: 25964785]

19. Koro C, Hellvard A, Delaleu N, Binder V, Scavenius C, Bergum B, Głowczyk I, Roberts HM, Chapple ILC, Grant MM, Rapala-Kozik M, Klaga K, Enghild JJ, Potempa J, Mydel P. Carbamylated LL-37 as a modulator of the immune response. Innate Immunity. 2016; 22(3):218–229. [PubMed: 26878866]

20. Ahmad-Nejad P, Häcker H, Rutz M, Bauer S, Vabulas RM, Wagner H. Bacterial CpG-DNA and lipopolysaccharides activate Toll-like receptors at distinct cellular compartments. European Journal of Immunology. 2002; 32(7):1958–1968. [PubMed: 12115616]

21. Nakagawa Y, Gallo RL. Endogenous Intracellular Cathelicidin Enhances TLR9 Activation in Dendritic Cells and Macrophages. Journal of Immunology. 2015; 194(3):1274–1284.

22. Spengler J, Lugonja B, Ytterberg AJ, Zubarev RA, Creese AJ, Pearson MJ, Grant MM, Milward M, Lundberg K, Buckley CD, Filer A, Raza K, Cooper PR, Chapple IL, Scheel-Toellner D. Release of Active Peptidyl Arginine Deiminases by Neutrophils Can Explain Production of Extracellular Citrullinated Autoantigens in Rheumatoid Arthritis Synovial Fluid. Arthritis Rheumatology. 2015; 67(12):3135–3145. [PubMed: 26245941]

23. Hao G, Wang D, Gu J, Shen Q, Gross SS, Wang Y. Neutral loss of isocyanic acid in peptide CID spectra: a novel diagnostic marker for mass spectrometric identification of protein citrullination. Journal of the American Society for Mass Spectrometry. 2009; 20(4):723–727. [PubMed: 19200748]

24. Garcia-Romo GS, Caielli S, Vega B, Connolly J, Allantaz F, Xu Z, Punaro M, Baisch J, Guiducci C, Coffman RL, Barrat FJ, Banchereau J, Pascual V. Netting Neutrophils are Major Inducers of Type I IFN Production in Pediatric Systemic Lupus Erythematosus. Science Translational Medicine. 2011; 3(73):73ra20.

25. Knight JS, Subramanian V, O'-Dell AA, Yalavarthi S, Zhao W, Smith CK, Hodgin JB, Thompson PR, Kaplan MJ. Peptidylarginine deiminase inhibition disrupts NET formation and protects against kidney, skin and vascular disease in lupus-prone MRL/lpr mice. Annals of the Rheumatic Diseases. 2014; 74(12):2199–2206. [PubMed: 25104775]

26. Kahlenberg JM, Carmona-Rivera C, Smith CK, Kaplan MJ. Neutrophil extracellular trap-associated protein activation of the NLRP3 inflammasome is enhanced in lupus macrophages. Journal of Immunology. 2012; 190:000–000.

27. Sadler AJ, Williams BRG. Interferon-inducible antiviral factors. Nature Reviews Immunology. 2008; 8:559–568.

28. Lande R, Ganguly D, Facchinetti V, Frasca L, Conrad C, Gregorio J, Meller S, Chamilos G, Sebasigari R, Riccieri V, Bassett R, Amuro H, Fukuhara S, Ito T, Liu YJ, Gilliet M. Neutrophils

activate Plasmacytoid Dendritic Cells by releasing self-DNA-peptide Complexes in Systemic Lupus Erythematosus. Science Translational Medicine. 2011; 9:3(73):73ra19.

29. Bauer S. Toll-erating self DNA. Nature Immunology. 2006; 7:13–15. [PubMed: 16357851]

30. Chamilos G, Gregorio J, Meller S, Lande R, Kontoyiannis DP, Modlin RL, Gilliet M. Cytosolic Sending of Extracellular self-DNA Transported into Monocytes by the Antimicrobial Peptide LL37. Blood. 2012; 120(18):3699–3707. [PubMed: 22927244]

31. Neumann A, Völlger L, Berends ETM, Molhoek EM, Stapels DAC, Midon M, Fri es A, Pingoud A, Rooijakkers SHM, Gallo RL, Mörgelin M, Nizet V, Naim HY, Köckritz-Blickwede MV. Novel role of the antimicrobial peptide LL-37 in the protection of neutrophil extracellular traps against degradation by bacterial nucleases. Journal of Innate Immunology. 2014; 6(6):860–868.

32. Khandpur R, Carmona-Rivera C, Vivekanandan-Giri A, Gizinski A, Yalavarthi S, Knight JS, Friday S, Li S, Patel RM, Subramanian V, Thompson P, Chen P, Fox DA, Pennathur S, Kaplan MJ. NETs are a source of citrullinated autoantigens and stimulate inflammatory responses in rheumatoid arthritis. Sci Transl Med. 2014; 5(178):178ra40.

33. Parker H, Albrett AM, Kettle AJ, Winterbourn CC. Myeloperoxidase associated with neutrophil extracellular traps is active and mediates bacterial killing in the presence of hydrogen peroxide. Journal of Leukocyte Biology. 2012; 91(3):369–376. [PubMed: 22131345]

34. Clement CC, Moncrieffe H, Lele A, Janow G, Becerra A, Bauli F, Saad FA, Perino G, Montagna C, Cobelli N, Hardin J, Stern LJ, Ilowite N, Porcelli SA, Santambrogio L. Autoimmune response to transthyretin in juvenile idiopathic arthritis. JCI Insight. 2016; 1(2):e85633. [PubMed: 26973882]

35. Schuster S, Hurrell B, Tacchini-Cottier F. Crosstalk between Neutorphils and Dendritic Cells: a context-dependent process. Journal of Leukocyte Biology. 2013; 94(4):671–675. [PubMed: 23250891]

36. Suzuki A, Yamada R, Yamamoto K. Citrullination by Peptidylarginine Deiminase in Rheumatoid Arthritis. Annals of the New York Academy of Sciences. 2007; 1108:323–339. [PubMed: 17893996]

37. Wang S, Wang Y. Peptidylarginine Deiminases in Citrullination, Gene Regulation, Health and Pathogenesis. Biochimica et Biophysica Acta. 2013; 1829(10):1126–1135. [PubMed: 23860259]

38. Shevchenko A, Tomas H, Havlis J, Olsen JV, Mann M. In-gel digestion for mass spectrometric characterization of proteins and proteomes. Nature protocols. 2006; 1(6):2856–2860. [PubMed: 17406544]

39. Knight JS, Zhao W, Luo W, Subramanian V, O'Dell AA, Yalavarthi S, Hodgin JB, Eitzman DT, Thompson PR, Kaplan MJ. Peptidylarginine deiminase inhibition is immunomodulatory and vasculoprotective in murine lupus. Journal of Clinical Investigation. 2013; 123(7):2891–2993.

40. Bicker KL, Subramanian V, Chumanevich AA, Hofseth LJ, Thompson PR. Seeing Citrulline: Development of a Phenylglyoxal-Based Probe to Visualize Protein Citrullination. J Am Chem Soc. 2012; 134(41):17015–17018. [PubMed: 23030787]

41. Balakrishnan S, Scheuermann MJ, Zondlo NJ. Arginine mimetics using α-guanidino acids: introduction of functional groups and stereochemistry adjacent to recognition guanidiniums in peptides. Chembiochem. 2012; 13(2):259–270. [PubMed: 22213184]
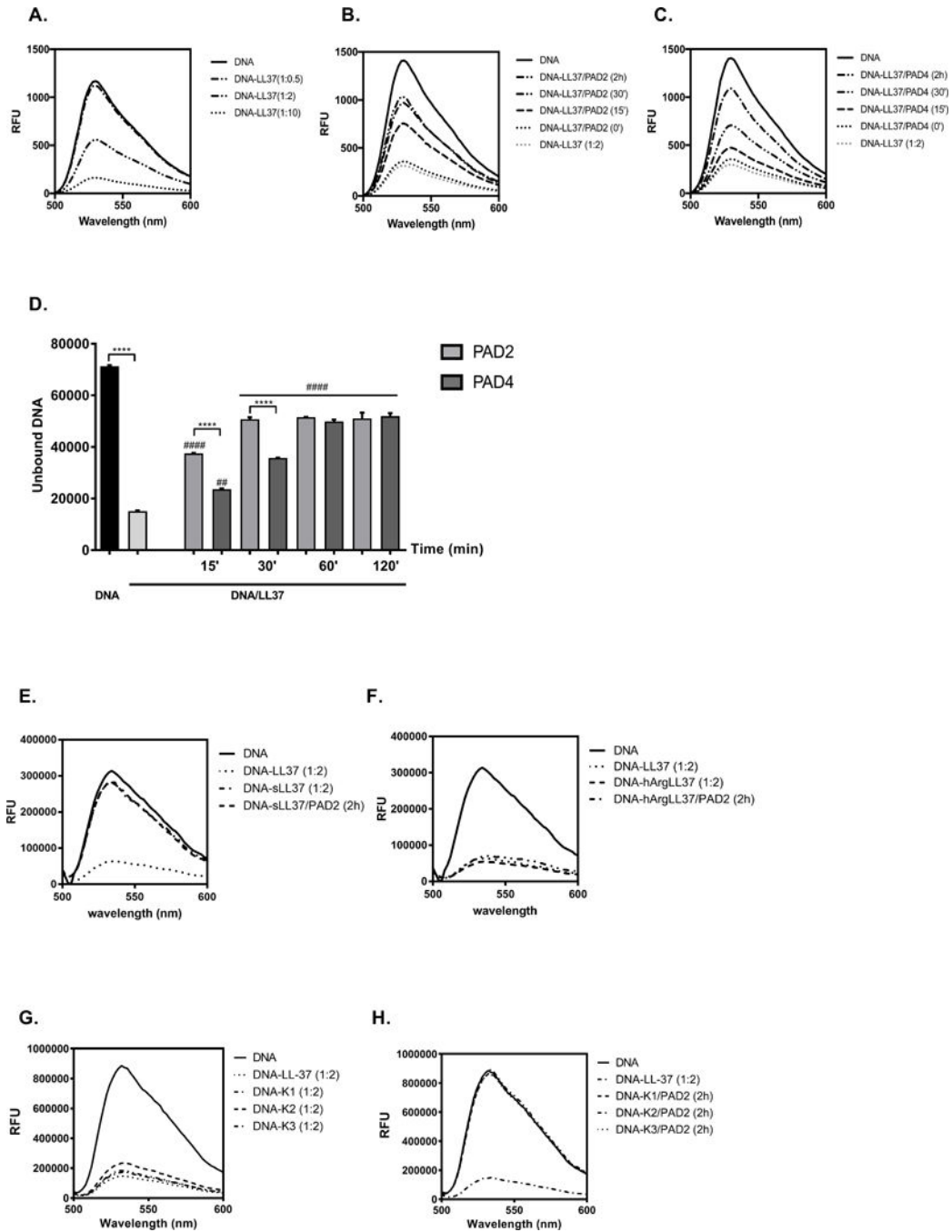
Figure 1. The influence of LL-37 citrullination on DNA binding

(**A**) The optimal binding between DNA and LL-37 was established by incubation of molecules at the different molar ratio of 1:0.5, 1:2, 1:10 (DNA:peptide) for 10 min at room temperature. Unbound DNA was quantified with spectral analysis using PicoGreen and is shown as relative fluorescence units (RFU). (**B, C, D**) The time dependent effect of LL-37 incubation with PAD2 (B) and PAD4 (C) on peptide capability to bind DNA. Statistical significance was evaluated by one-way ANOVA, followed by Tukey's multiple comparisons post-test (****$p<0.000$ – comparing to control; ##$p<0.01$; ####$p<0.0001$- comparing with

DNA/LL-37). (**E**) The DNA binding to the untreated scrambled peptide (sLL37) and after its citrullination with PAD2. (**F**) The DNA binding by LL-37 with Arg residues substituted with homoarginine (hArg-LL-37) with or without pretreatment with PAD2. (**G**) The binding of carbamylated variants of LL-37 to DNA before and after (**H**) preincubation with PAD2.
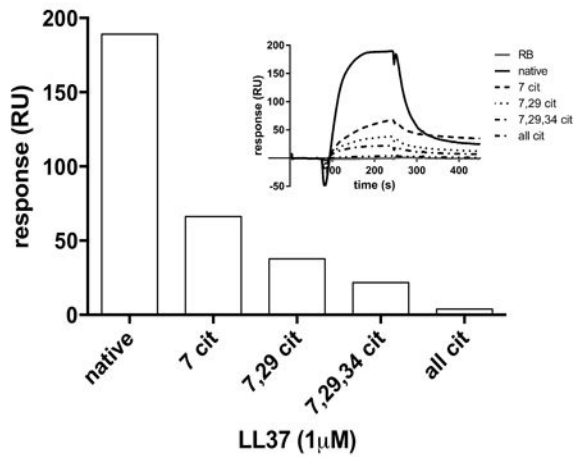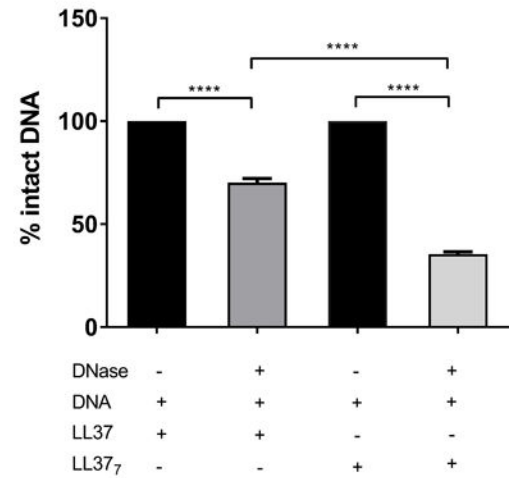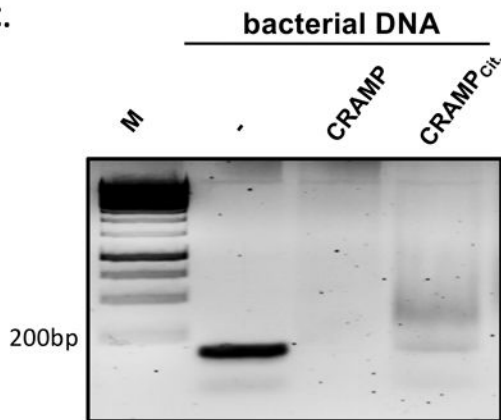
Figure 2. The characterization of DNA binding by variably citrullinated forms of LL-37
(**A**) The efficiency of DNA binding by native and differentially citrullinated forms of LL-37 (LL-37$_7$, LL-37$_{7,29}$, LL-37$_{7,29,34}$, and fully citrullinated LL-37) estimated with surface plasmon resonance analysis. Response units (RU) were used to describe the amounts of coupled DNA. (**B**) The efficiency of modified LL-37 to protect DNA against degradation represented as the percentage of DNA bound to the peptide after 60 min of DNase treatment. Statistical significance was evaluated by one-way ANOVA, followed by Tukey's multiple comparisons post-test (****$P<0.0001$). (**C**) Citrullination of CRAMP affects the peptide binding to bacterial DNA visualised by retardation assay.
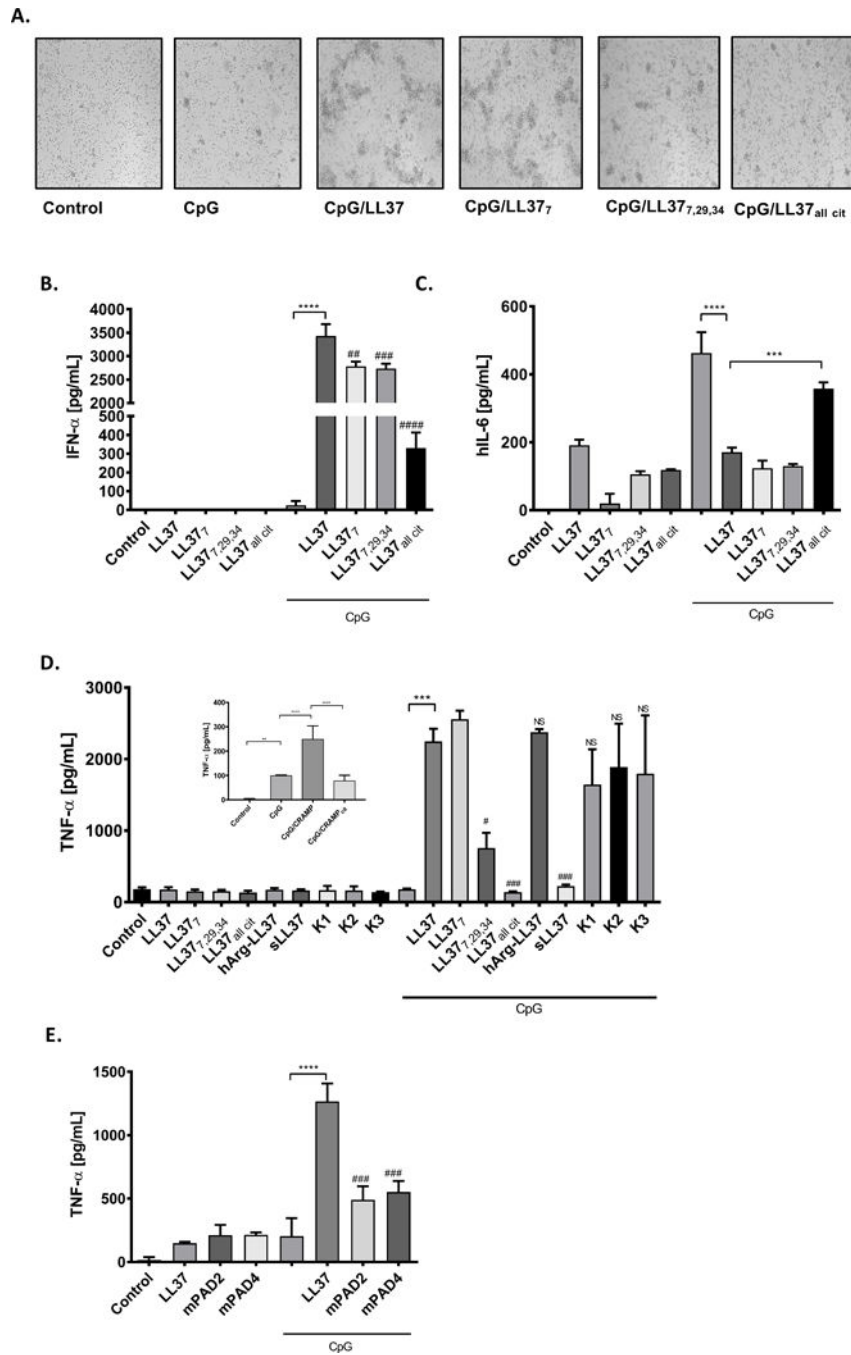
Figure 3. The biological effects of LL-37 citrullination on phagocytes

Primary human pDCs or murine macrophages cell line (RAW 264.7) were incubated with CpG (3 mM) or CpG combined with differentially citrullinated LL-37 forms (28.8 mg/mL) for 15 min. Thereafter cells were washed 3 times with PBS and incubated in fresh medium for additional 20 h. (**A**) Formation of cell clumps reflecting the activation of human pDCs; (**B**) IFN-α and (**C**) IL-6 levels measured by ELISA in culture supernatant. Statistical significance was evaluated by one-way ANOVA, followed by Tukey's multiple comparisons post-test (***$P<0.001$, ****$P<0.0001$- comparing to control; ##$P<0.01$, ###$P<0.001$,

####P<0.0001, comparing with CpG-LL37). (**D**) The expression of TNF-α in murine macrophages upon exposition to CpG alone, CpG with human synthetic native and different modified forms of LL-37 or CpG with murine native and citrullinated cathelicidin (CRAMP) – insert. TNF-α secretion to the culture supernatant was measured with ELISA. Statistical significance was evaluated by one-way ANOVA, followed by Tukey's multiple comparisons post-test (**P<0.01, ***P<0.001, ****P<0.0001; compared to control; #P<0.05, ###P<0.001, compared with CpG-LL37). (**E**) Raw 264.7 were stimulated with CpG (10uM) alone or with mixtures of peptides (mPAD2 and mPAD4) that resemble the catalytic modification of LL-37 by PAD2 and PAD4, respectively. TNF-α production in the culture supernatant was measured with ELISA. Statistical significance was evaluated by one-way ANOVA, followed by Tukey's multiple comparisons post-test (****P<0.0001 – compared to control; ###P<0.001, compared to CpG-LL37).
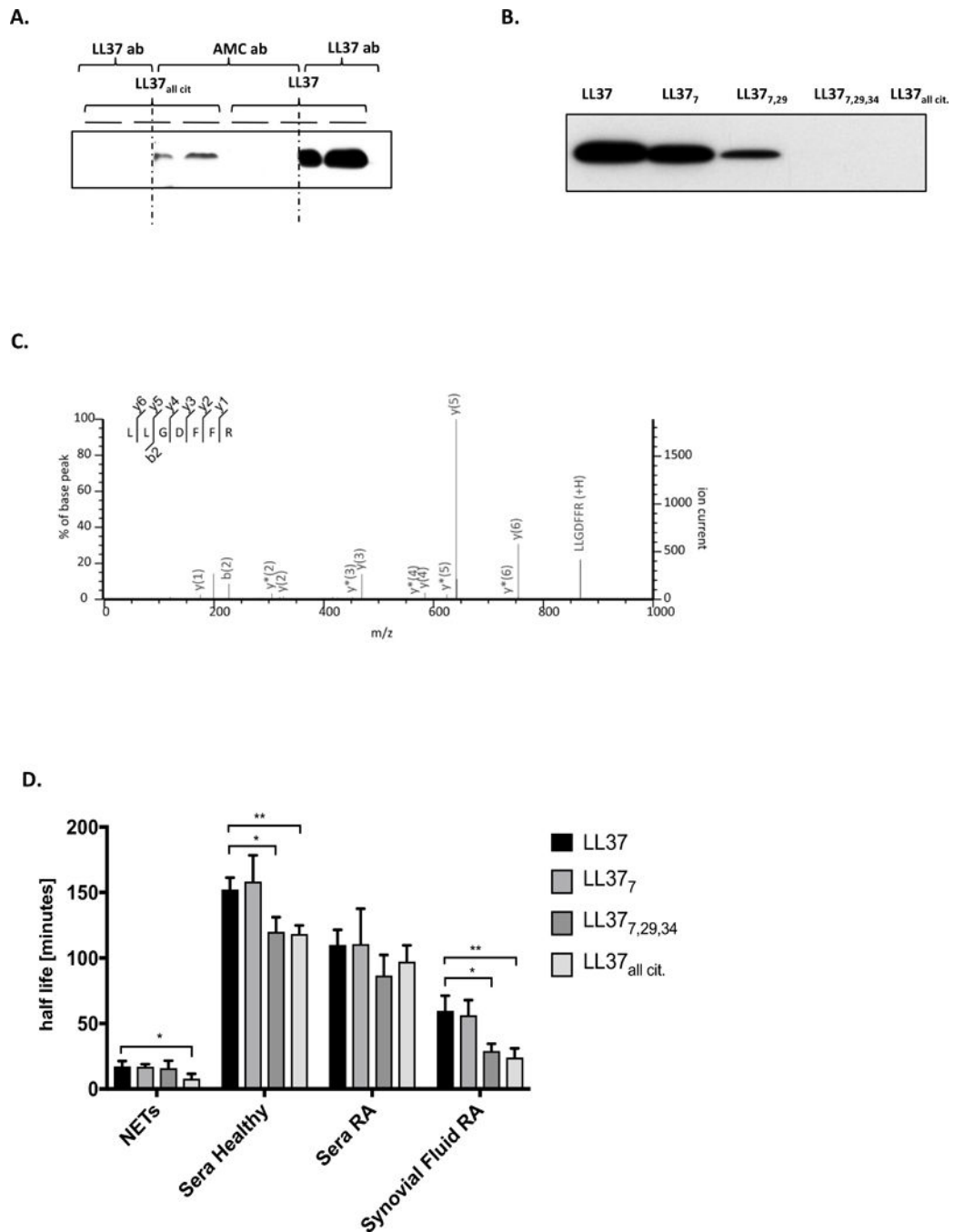
Figure 4. Identification of citrullinated LL-37

(**A**) Western Blot analysis of native and fully-citrullinated LL-37 using antibodies against native LL-37 (LL-37 ab) and anti-modified citrulline proteins (AMC ab). The red dashed line showed the section where the membrane was cut to allow the incubation of different antibodies as described previously. (**B**) Western Blot verification of the recognition of differentially citrullinated forms of LL-37 by antibodies against native LL-37. (**C**) MSMS spectra of LL-37 N-terminal tryptic peptide (LLGDFFR), confirming the presence of mature LL-3. (**D**) The half-life of native LL-37 and its variably citrullinated forms in NETs, healthy

and inflamed sera (RA serum) and synovial fluid of rheumatoid arthritis patients. Unpaired t-test was used to calculate the p values between groups (*=p<0.05).
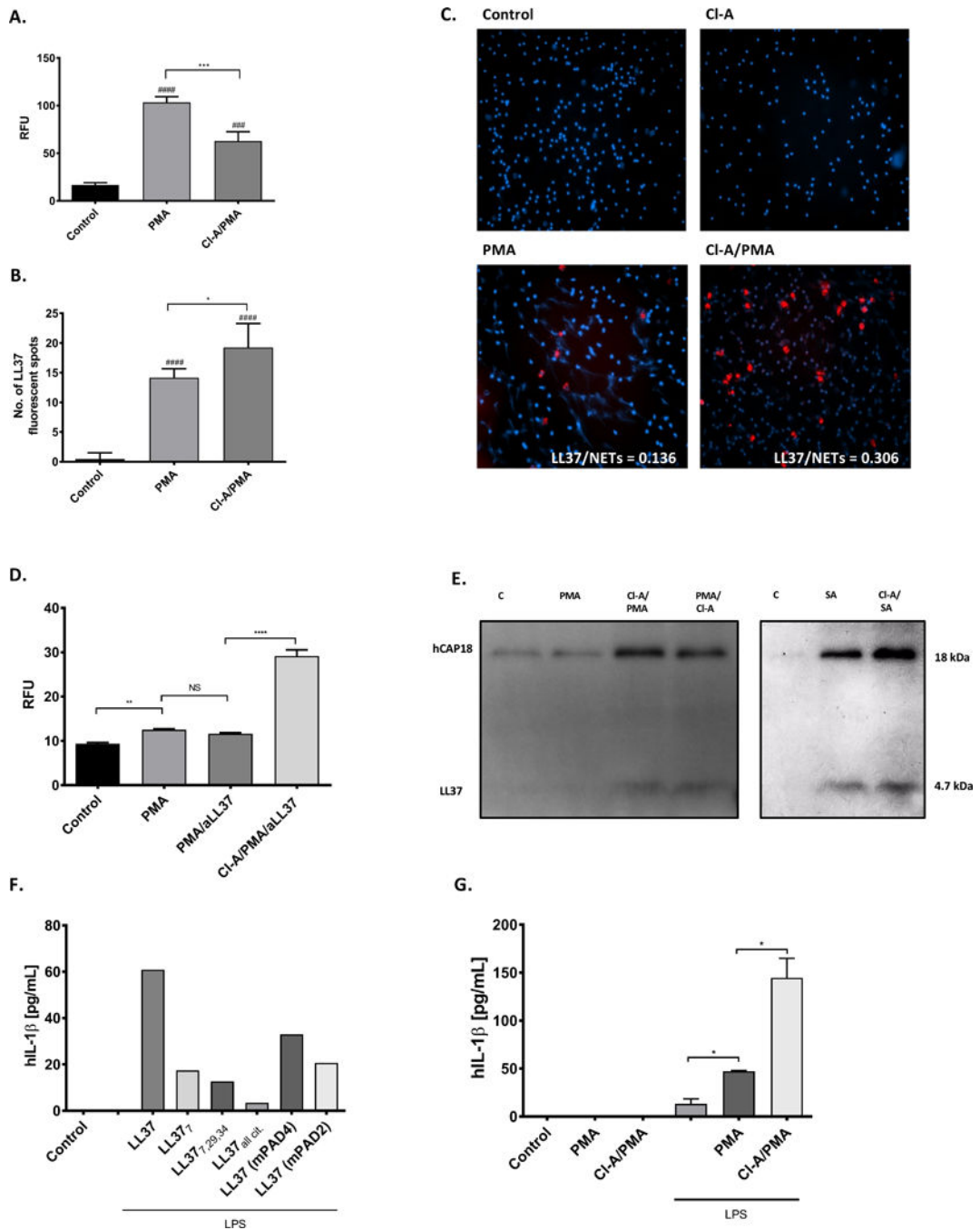
Figure 5. The citrullination of LL-37 in NETs

Human neutrophils were treated either with or without 100 μM Cl-Amidine (Cl-A) for 1h prior stimulation with 25 nM PMA for 3 h. Sham-treated neutrophils constituted a background control. (**A**) Formation of NETs quantified using PicoGreen and is shown as relative fluorescence units (RFU). (**B, C**) The presence of LL-37 visualized by fluorescent microscopy using Alexa Fluor 647-labelled antibody against human LL-37 (red) and counterstained with Hoechst (blue). The representative images taken at the magnification ×20 (**C**). Fluorescence from single molecule of LL-37 is imaged as spots and quantification

of the red fluorescent signals is from 20 independent images (**B**). Statistical significance was evaluated by one-way ANOVA, followed by Tukey's multiple comparisons post-test (*$P<0.05$, ***$P<0.001$ – compared with control; ###$P<0.001$, ####$P<0.0001$, compared with Control). (**D**) Neutrophils from healthy donors were stimulated as indicated. Anti-LL37 was added 2 h post PMA activation. Supernatants were collected and formation of NETs was quantified using PicoGreen. Statistical significance was evaluated by one-way ANOVA, followed by Tukey's multiple comparisons post-test (**$P<0.01$). (**E**) The identification of the LL-37 mature peptide (LL-37 – 4.7 kDa) and its precursor (hCAP18 – 18 kDa) in NETs generated in presence/absence of 100 μM Cl-A and PMA (25 nM) or *Staphylococcus aureus* (MOI 1:10) using Western blot analysis with antibodies against native LL-37. (**F, G**) Human macrophages were primed with or without LPS for 4 h, then treated with synthetic native and differentially citrullinated forms of LL-37 (LL-37$_7$, LL-37$_{7,29}$, LL-37$_{7,29,34}$, and fully citrullinated LL-37) and peptide mixtures resembles the catalytic modification of LL-37 by PAD2 (mPAD2) and PAD4 (mPAD4) (**F**) or NETs collected from PMA-activated neutrophils as described previously (**G**) for 2h. Supernatants were collected and secretion of IL-1β was quantified by commercialized ELISA. Unpaired t-test was used to calculate the *p* values between groups (*=p<0.05).
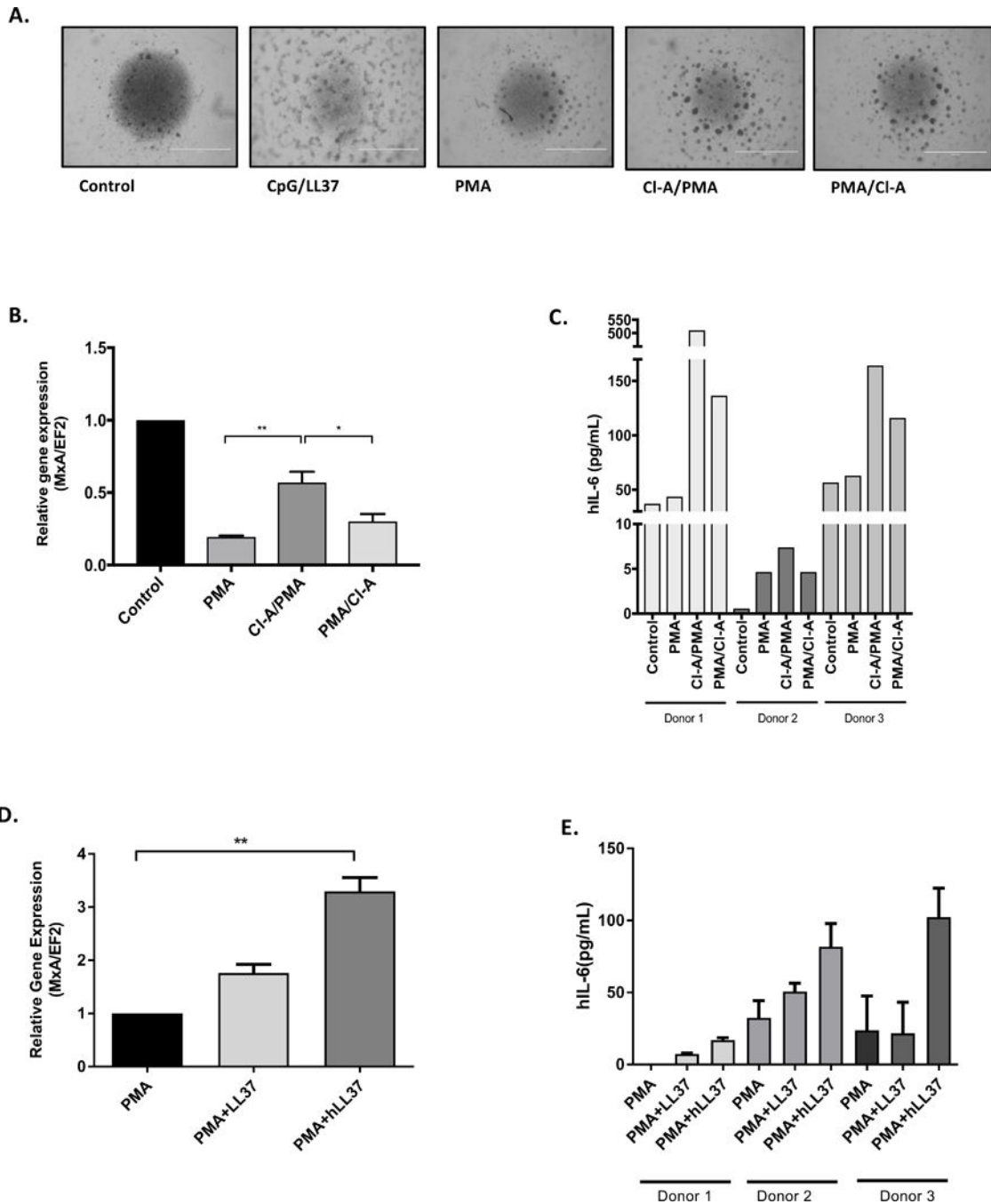
Figure 6. The activation of pDCs by NETs with differential content of citrullinated proteins
pDCs were exposed to NETs collected from PMA-activated neutrophils and neutrophils additionally exposed to Cl-A (Cl-A/PMA – 1 h preincubation of PMN with Cl-A before PMA; PMA/Cl-A – Cl-A was added 2 h post PMA stimulation). (**A**) The morphology of the cell clumps formation triggered with NETs collected from PMA-activated neutrophils pre-treated with or without Cl-A. (**B**) The level of *MxA* gene expression in pDCs measured by real-time PCR. (**C**) Production of IL-6 cytokine measured with ELISA in supernatants collected from pDCs. (**D, E**) The activation of pDCs by NETs supplemented with LL37 and

hArg-LL37 estimated by the level of MxA gene expression (**D**) and amount of secreted IL-6 in conditioned media (**E**). Statistical significance was evaluated by one-way ANOVA, followed by Tukey's multiple comparisons post-test (*P<0.05, **P<0.01).

Table I

Sequences of LL-37 used in the study.

Peptide	Sequence
LL-37	LLGDFFRKSKEKIGKEFKRIVQRIKDFLRNLVPRTES
LL-37$_7$	LLGDFF(**Cit**)KSKEKIGKEFKRIVQRIKDFLRNLVPRTES
LL-37$_{7,29}$	LLGDFF(**Cit**)KSKEKIGKEFKRIVQRIKDFL(**Cit**)NLVPRTES
LL-37$_{7,29,34}$	LLGDFF(**Cit**)KSKEKIGKEFKRIVQRIKDFL(**Cit**)NLVP(**Cit**)TES
LL-37$_{all\ cit.}$	LLGDFF(**Cit**)KSKEKIGKEFK(**Cit**)IVQ(**Cit**)IKDFL(**Cit**)NLVP(**Cit**)TES
LL-37$_{K1}$	LLGDFFR(**ε-carb-K**)SKEKIGKEFKRIVQRIKDFLRNLVPRTES
LL-37$_{K2}$	LLGDFFRKSKE(**ε-carb-K**)IG(**ε-carb-K**)EFKRIVQRIKDFLRNLVPRTES
LL-37$_{K3}$	LLGDFFRSKEKIGKEFKRIVQRI(**ε-carb-K**)DFLRNLVPRTES
sLL-37	RSLEGTDRFPFVRLKNSRKLEFKDIKGIKREQFVKIL
hLL-37	LLGDFF(**hR**)KSKEKIGKEFK(**hR**)IVQ(**hR**)IKDFL(**hR**)NLVP(**hR**)TES
CRAMP	GLLRKGGEKIGEKLKKIGQKIKNFFQKLVPQPEQ
CRAMP$_{cit.}$	GLL(**Cit**)KGGEKIGEKLKKIGQKIKNFFQKLVPQPEQ

ε-carb-K: lysine carbamylated on the ε-carbon.

hR: homoarginine (hArg)